Supporting Information

Revealing the Effect of Sodium on Iron-Based Catalysts for CO_2 Hydrogenation: Insights from Calculation and Experiment

*Xianglin Liu[1], Chao Zhang[1], Pengfei Tian[2], Minjie Xu[1], Chenxi Cao[1], Zixu Yang[1], Minghui Zhu[1], Jing Xu[1],**

[1]State Key Laboratory of Chemical Engineering, School of Chemical Engineering, East China University of Science and Technology, Shanghai 200237, China

[2]School of Mechanical and Power Engineering, East China University of Science and Technology, Shanghai 200237, China

Corresponding author

Jing Xu - *State Key Laboratory of Chemical Engineering, School of Chemical Engineering, East China University of Science and Technology, No.130 Meilong Road, Shanghai 200237, China; E-mail: xujing@ecust.edu.cn*

Contents of the Supporting Information

Number of Pages	Pages(S1-S16)
Number of Figures	20 Figures
Number of Tables	3 Tables

The crystal sizes of Fe_5C_2 were calculated by the Debye-Scherrer equation (S1) using MDI Jade 5.0 software.

$$D = \frac{0.9\lambda}{\Delta \cos\theta} \tag{S1}$$

Where D is the crystal size, λ is the wavelength of X-rays, △ is the full width of half maximum (FWHM) of diffraction peak [(510) facet for Fe_5C_2], and θ is the angle corresponding to the peak (2θ = 44.28 °) in this paper.

The reaction rate was calculated according to the equation S2.

$$Rate = \frac{60 * Q_{in} * v_{CO_{2in}} * X_{CO_2}}{1000 * Vm} * \frac{M_{Fe_2O_3}}{2\mathrm{m}_{cat.}} \tag{S2}$$

Here, Q_{in} is the volume flow rate of the inlet stream (mL/min); $v_{CO_2\ \mathrm{in}}$ is the volume fraction of CO_2 in the inlet stream; X_{CO_2} is the conversion of CO_2; V_m is the molar volume of gas (mol/L); $M_{Fe_2O_3}$ is the molar mass of Fe_2O_3 (g/mol); $\mathrm{m}_{cat.}$ is the actual mass of catalysts (g).

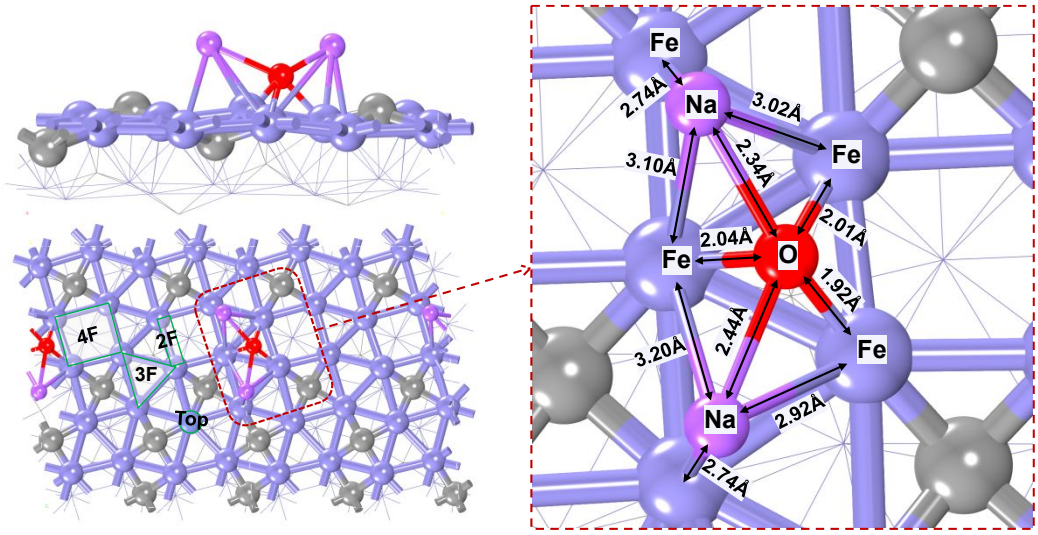

Figure S1. The energetically favorable configuration for the Na_2O on Fe_5C_2 (510) surface (The typical sites (Top, 2F, 3F and 4F) are marked) (Fe atoms in purple, C atoms in gray, O atoms in red, Na atoms in amaranth).

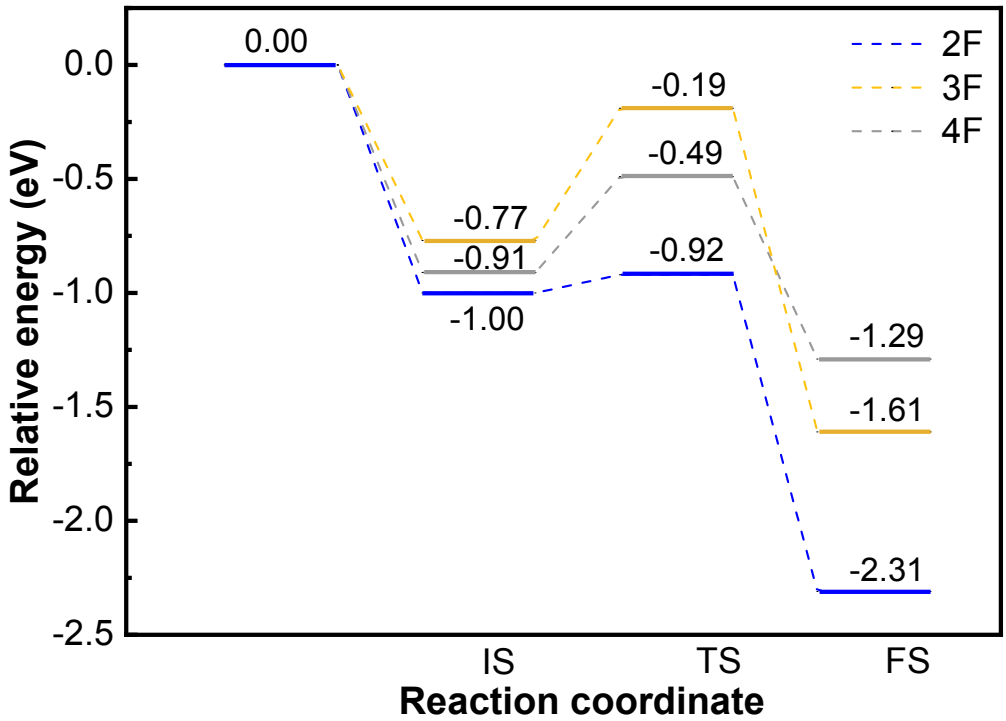

Figure S2. Energy profiles for CO_2 dissociation at typical sites on Na_2O/Fe_5C_2 (510) surface.

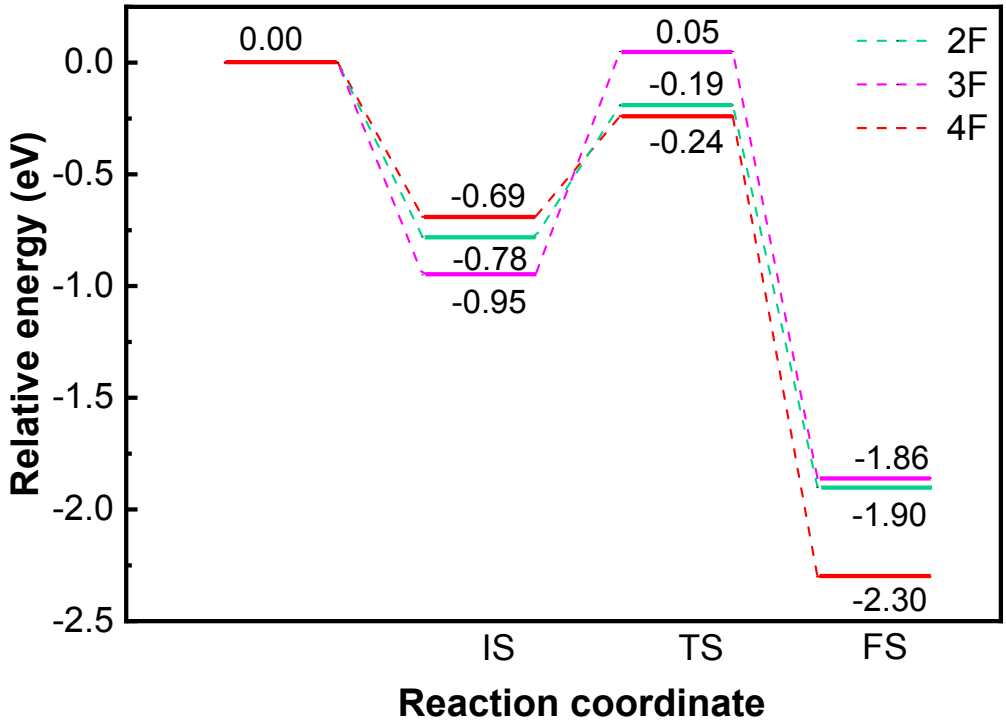

Figure S3. Energy profiles for CO_2 dissociation at typical sites on Fe_5C_2 (510) surface.

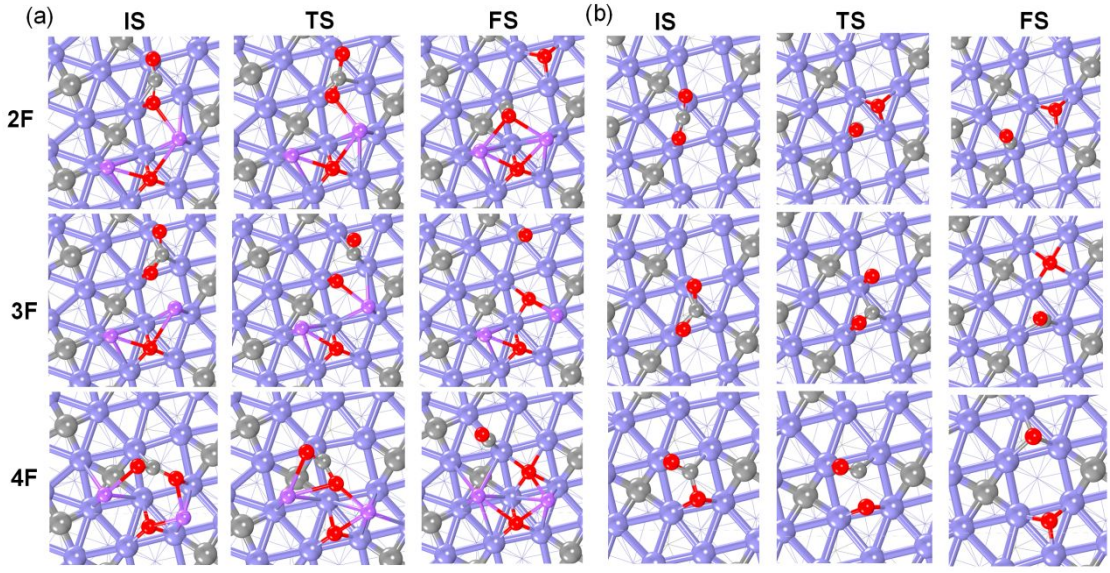

Figure S4. Corresponding configurations for CO_2 dissociation on (a) Na_2O/Fe_5C_2 (510) and (b) Fe_5C_2 (510) surfaces (Fe atoms in purple, C atoms in gray, O atoms in red, Na atoms in amaranth).

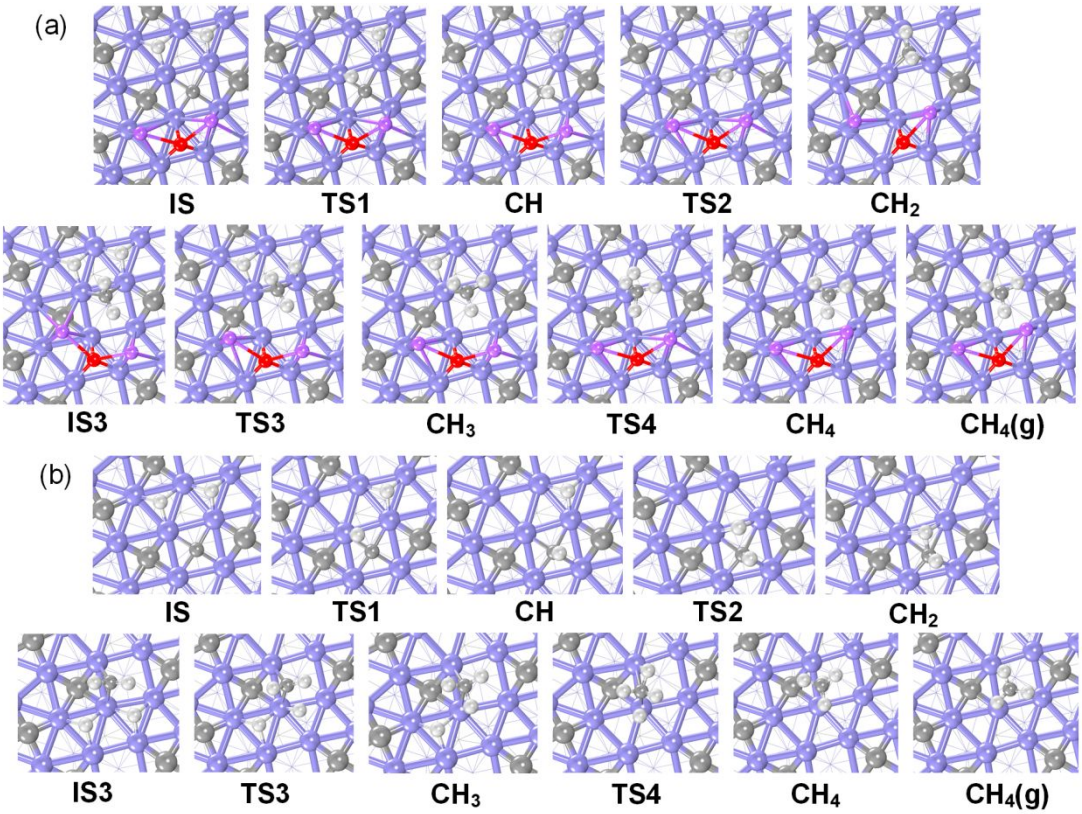

Figure S5. Corresponding configurations for CH_4 formation from C adatom on (a) Na_2O/Fe_5C_2 (510) and (b) Fe_5C_2 (510) surfaces (Fe atoms in purple, C atoms in gray, O atoms in red, Na atoms in amaranth, H atoms in hoar).

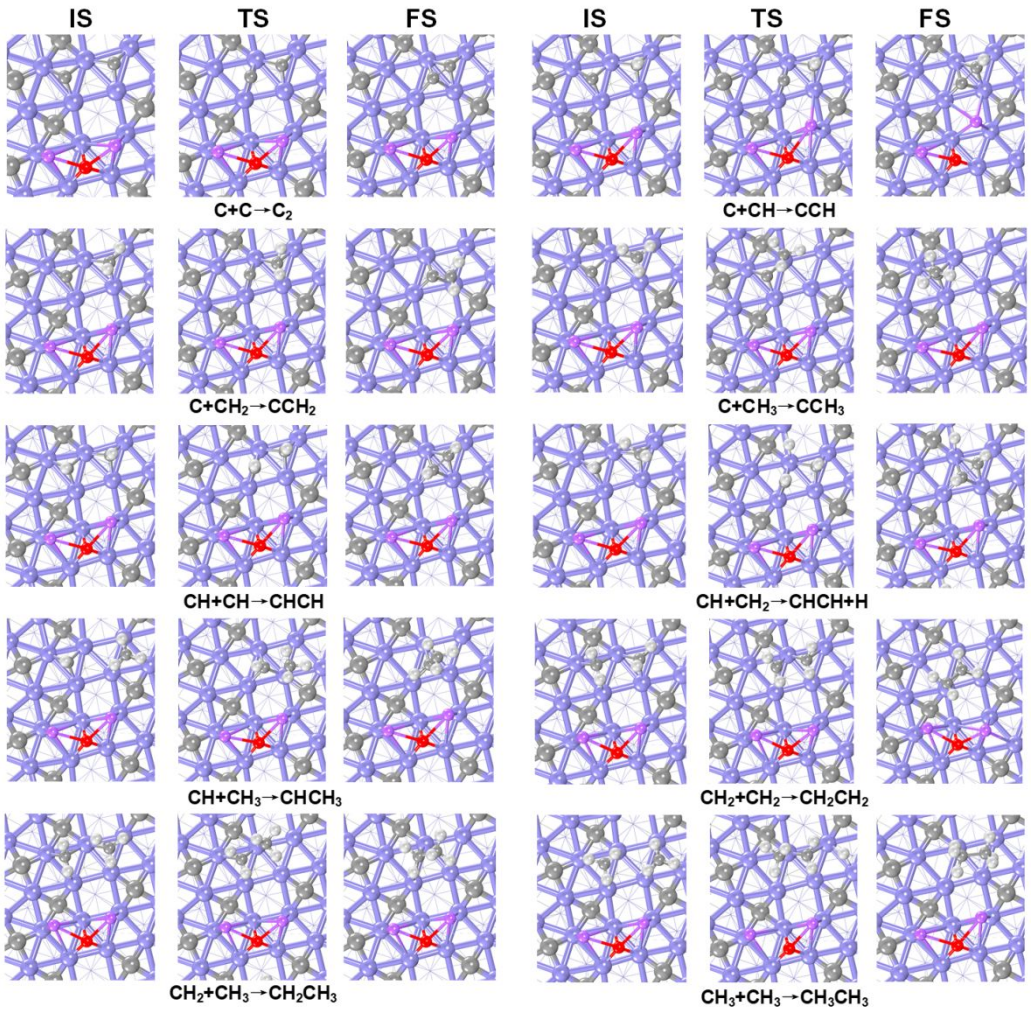

Figure S6. Corresponding configurations for C-C coupling reactions of CH_i intermediates on Na_2O/Fe_5C_2 (510) surface (Fe atoms in purple, C atoms in gray, O atoms in red, Na atoms in amaranth, H atoms in hoar).

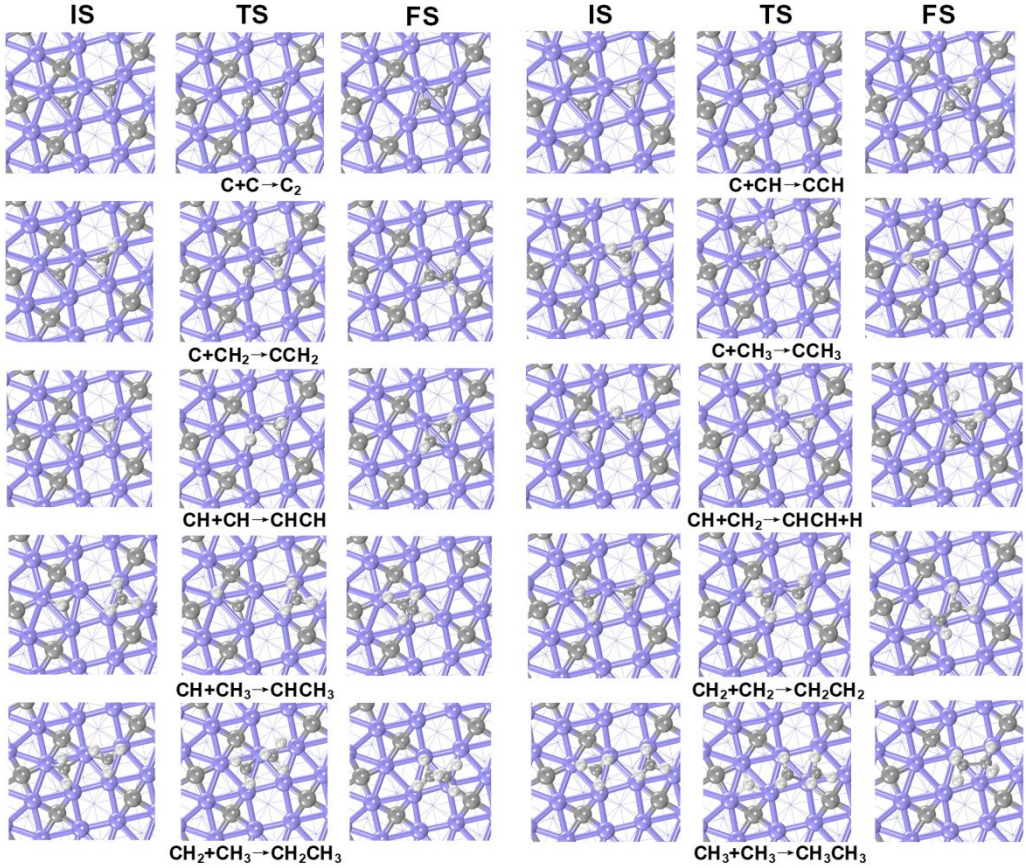

Figure S7. Corresponding configurations for C-C coupling reactions of CH_i intermediates on Fe_5C_2 (510) surface (Fe atoms in purple, C atoms in gray, O atoms in red, Na atoms in amaranth, H atoms in hoar).

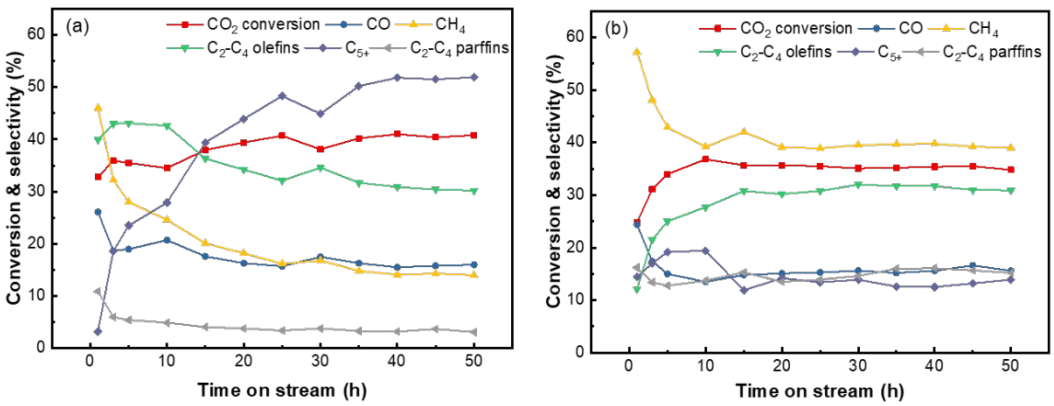

Figure S8. 50h time-on-stream reaction for 0.63%Na-Fe_2O_3 (a) and Na-free Fe_2O_3 (b) under industrial conditions (15000mL·g^{-1}·h^{-1}, 330 ℃, 1.5 MPa).

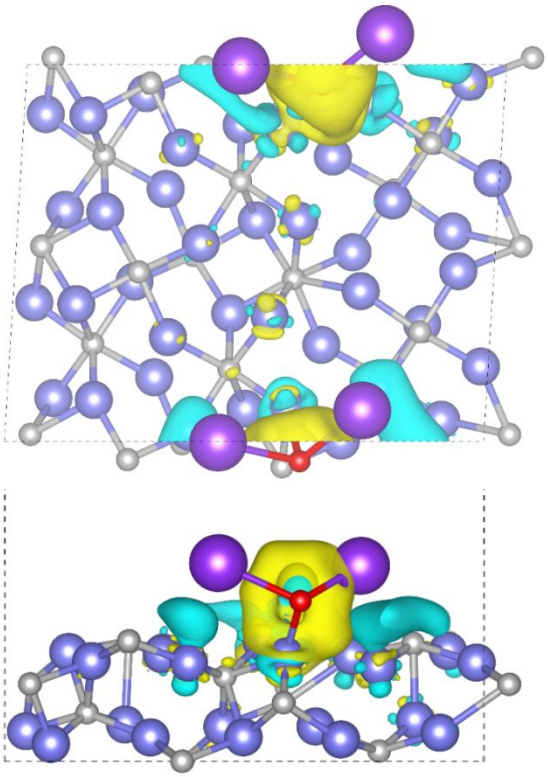

Figure S9. The charge density difference of Na_2O molecule for Na_2O/Fe_5C_2 (510) surface (yellow and cyan colors represent charge depletion and accumulation, respectively).

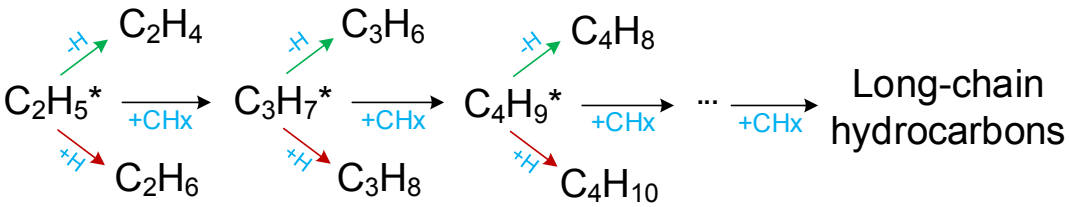

Figure S10. A simplified scheme of reaction mechanism for products.

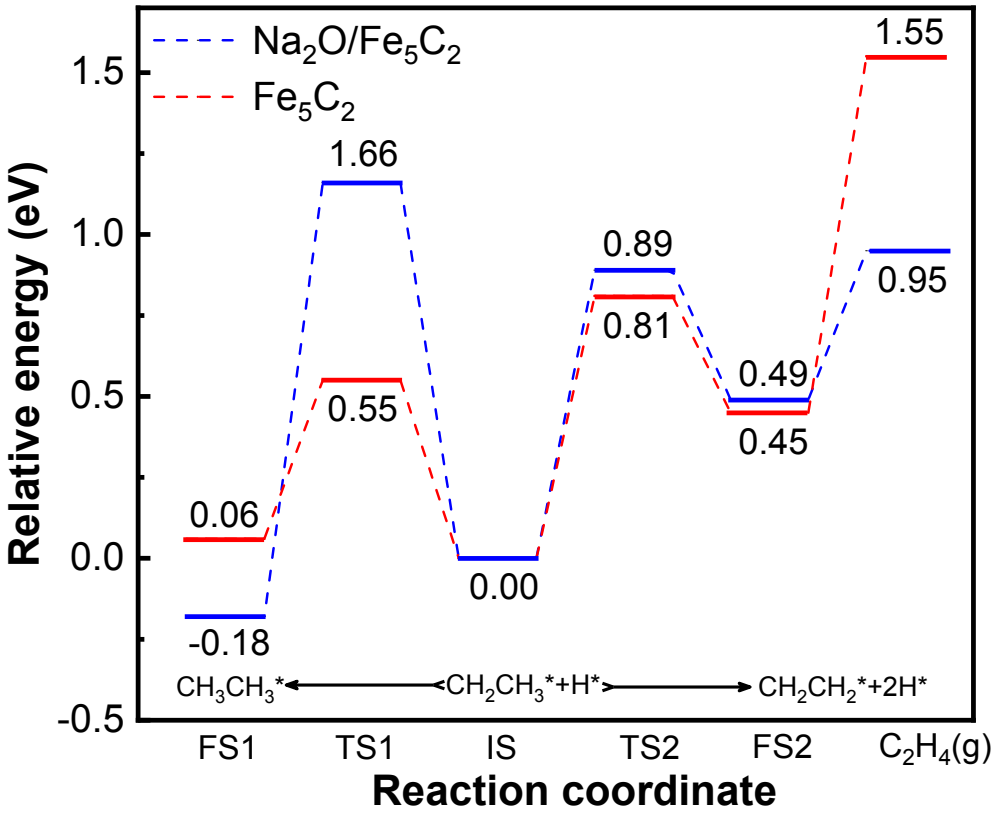

Figure S11. Energy profiles for C_2H_5 hydrogenation to C_2H_6 and dehydrogenation to C_2H_4 on Na_2O/Fe_5C_2 (510) (blue line) and Fe_5C_2 (510) (red line) surfaces.

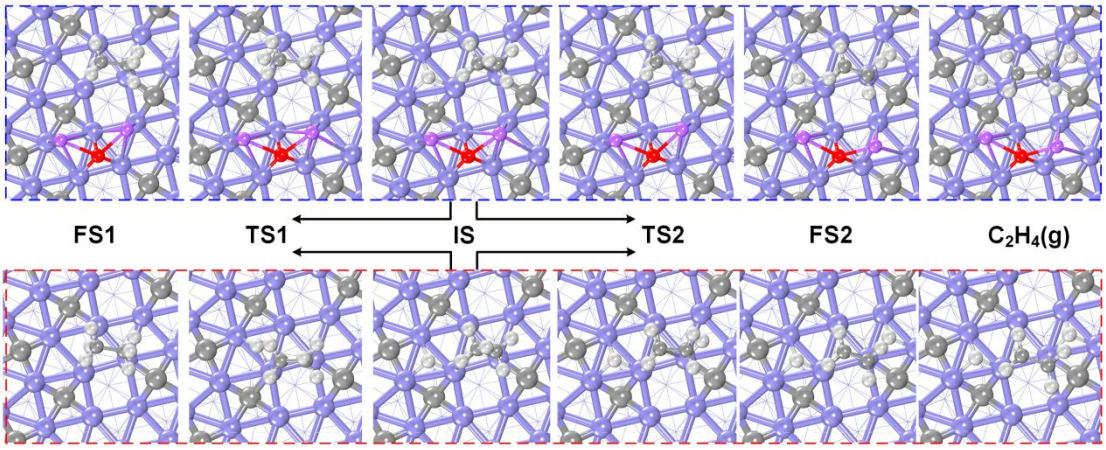

Figure S12. Corresponding configurations for the hydrogenation and dehydrogenation of ethyl on Na_2O/Fe_5C_2 (510) (blue dotted line) and Fe_5C_2 (510) (red dotted line) surfaces (Fe atoms in purple, C atoms in gray, O atoms in red, Na atoms in amaranth, H atoms in hoar).

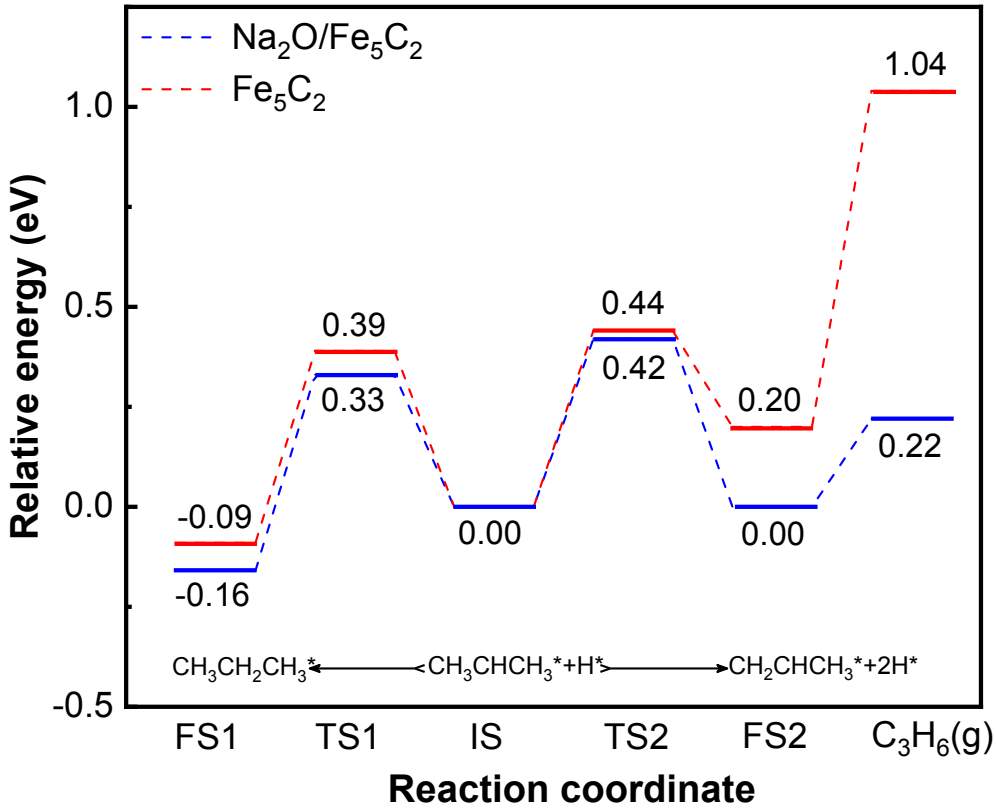

Figure S13. Energy profiles for C_3H_7 hydrogenation to C_3H_8 and dehydrogenation to C_3H_6 on Na_2O/Fe_5C_2 (510) (blue line) and Fe_5C_2 (510) (red line) surfaces.

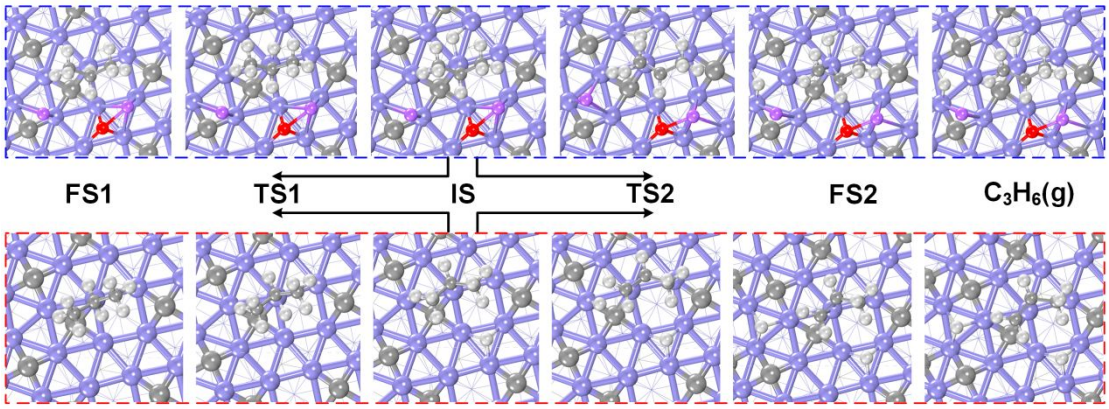

Figure S14. Corresponding configurations for the hydrogenation and dehydrogenation of propyl on Na_2O/Fe_5C_2 (510) (blue dotted line) and Fe_5C_2 (510) (red dotted line) surfaces (Fe atoms in purple, C atoms in gray, O atoms in red, Na atoms in amaranth, H atoms in hoar).

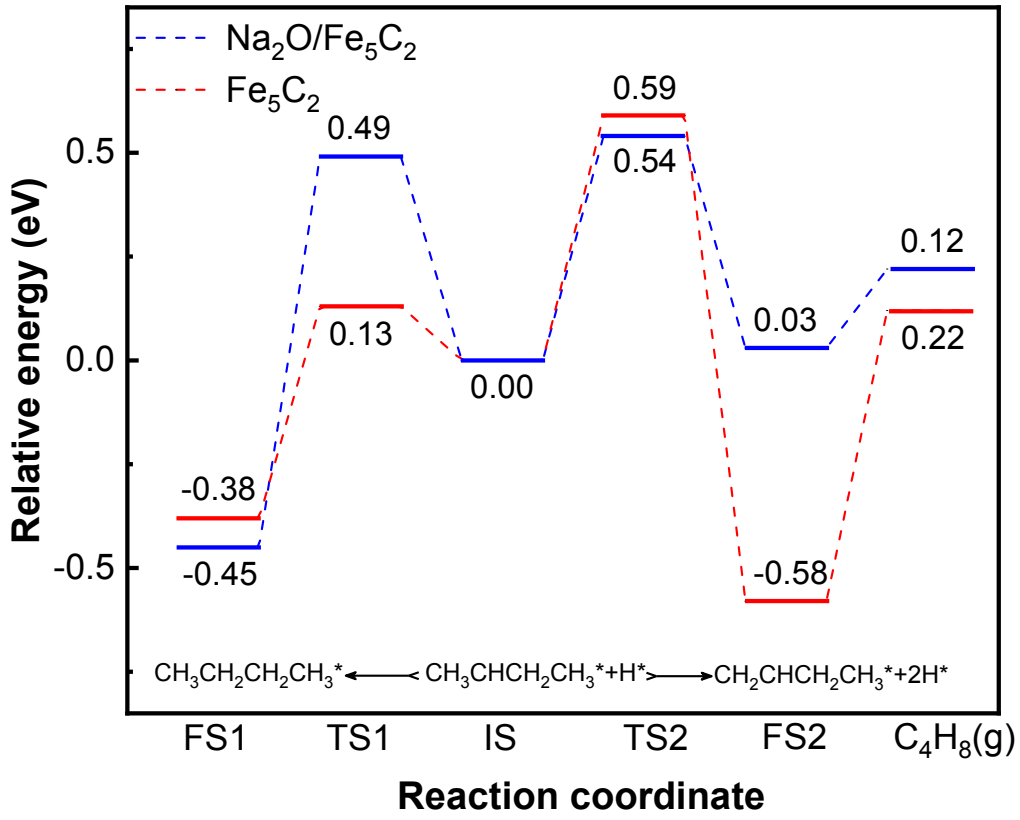

Figure S15. Energy profiles for C_4H_9 hydrogenation to C_4H_{10} and dehydrogenation to C_4H_8 on Na_2O/Fe_5C_2 (510) (blue line) and Fe_5C_2 (510) (red line) surfaces.

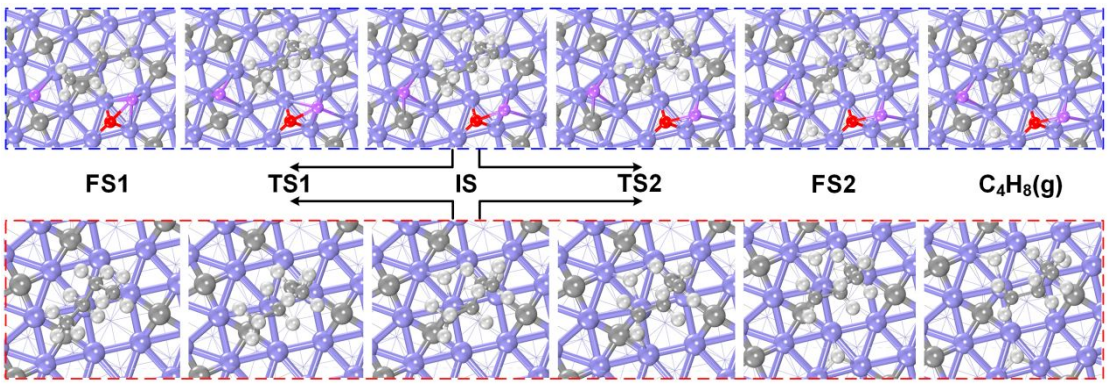

Figure S16. Corresponding configurations for the hydrogenation and dehydrogenation of butyl on Na_2O/Fe_5C_2 (510) (blue dotted line) and Fe_5C_2 (510) (red dotted line) surfaces (Fe atoms in purple, C atoms in gray, O atoms in red, Na atoms in amaranth, H atoms in hoar).

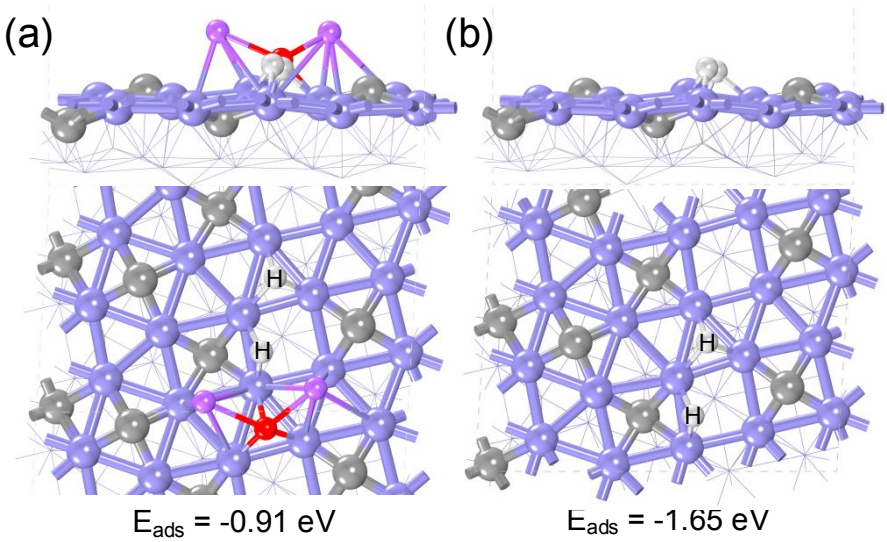

Figure S17. The optimized energetically favorable adsorption configurations of H_2 on (a) Na_2O/Fe_5C_2 (510) and (b) Fe_5C_2 (510) surfaces (Fe atoms in purple, C atoms in gray, O atoms in red, Na atoms in amaranth, H atoms in hoar).

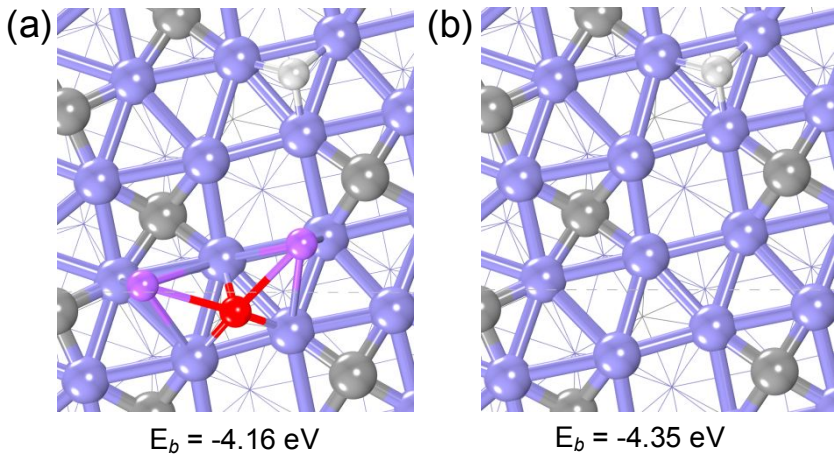

Figure S18. The binding energy and corresponding configurations of H adatom on (a) Na_2O/Fe_5C_2 (510) and (b) Fe_5C_2 (510) surfaces (Fe atoms in purple, C atoms in gray, O atoms in red, Na atoms in amaranth, H atoms in hoar).

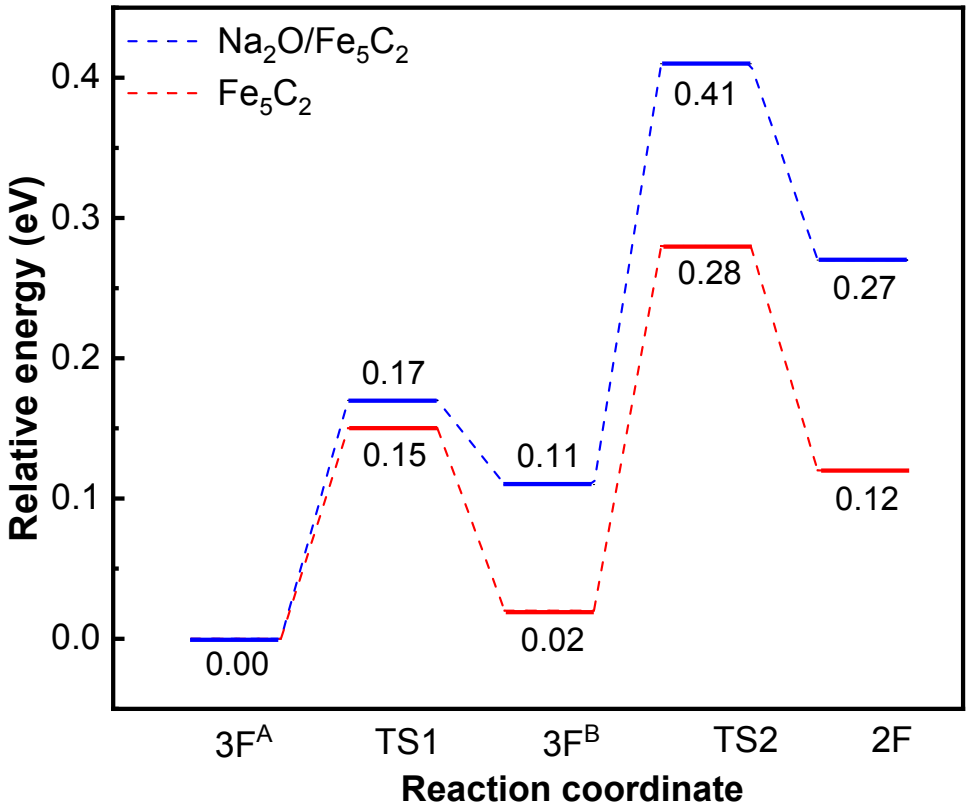

Figure S19. Energy profiles for the diffusion process of H adatom between different threefold hollow (3F) and twofold hollow (2F) sites on Na_2O/Fe_5C_2 (510) (blue line) and Fe_5C_2 (510) (red line) surfaces.

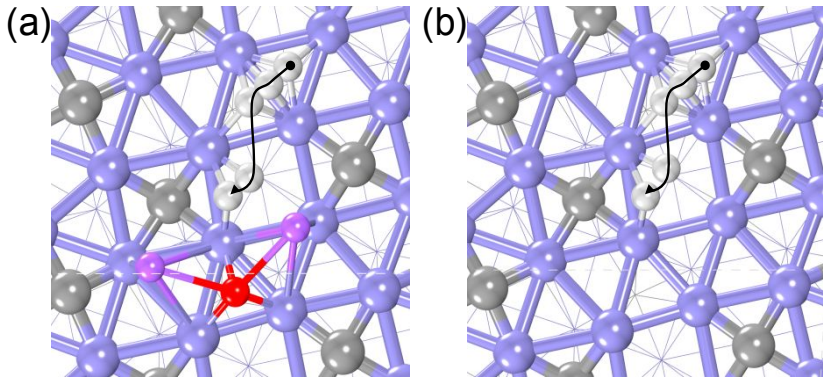

Figure S20. Corresponding configurations for the diffusion process of H adatom between different threefold hollow (3F) and twofold hollow (2F) sites on (a) Na_2O/Fe_5C_2 (510) and (b) Fe_5C_2 (510) surfaces (Fe atoms in purple, C atoms in gray, O atoms in red, Na atoms in amaranth, H atoms in hoar).

Table S1. The reaction energy barriers for all the calculated chain growth and CH_i intermediates hydrogenation reactions on Na_2O/Fe_5C_2 (510) and Fe_5C_2 (510) surfaces.

Ea	Na_2O/Fe_5C_2 (510)				Fe_5C_2 (510)			
	C	**CH**	**CH_2**	**CH_3**	**C**	**CH**	**CH_2**	**CH_3**
H	1.06	0.88	0.70	0.59	1.00	0.95	0.33	0.68
C	1.20	0.74	1.00	0.92	1.18	0.79	0.98	0.64
CH	0.74	0.56	0.39	1.07	0.79	0.62	0.41	1.20
CH_2	1.00	0.39	0.49	0.87	0.98	0.41	0.42	0.74
CH_3	0.92	1.07	0.87	1.18	0.64	1.20	0.74	1.19
ΔE_{CHi}	0.32	0.49	0.31	-0.28	0.36	0.54	-0.08	0.04

Table S2. ^{57}Fe Mössbauer parameters of the activated 0.63%Na-Fe_2O_3 and Na-free Fe_2O_3 catalysts.

Catalysts	Phase compositions		Mössbauer parameters			Area (%)
			IS (mm/s)	QS (mm/s)	Hhf (kOe)	
Activated 0.63%Na-Fe_2O_3	Fe_5C_2	Ⅰ	0.22	-0.08	210.3	45.9
		Ⅱ	0.2	0	188.1	38.9
		Ⅲ	0.19	0.05	109.8	15.2
Activated Na-free Fe_2O_3	Fe_5C_2	Ⅰ	0.25	-0.08	215.1	37.9
		Ⅱ	0.18	-0.05	184.1	46.9
		Ⅲ	0.20	-0.15	108.9	15.2

Table S3. The performance of Na promoted Fe-based catalysts for CO_2 hydrogenation

Catalysts	X_{CO_2} (%)	S_{C_i} (%) (Exclude CO)			O/P	S_{CO} (%)	Temp. (℃)	Pressure (MPa)	Ref.
		CH_4	C_2-C_4=	C_{5+}	C_2-C_4				
0.63%Na-Fe_2O_3	41.0	14.1	30.9	51.8	9.7	15.5	330	1.5	This work
Fe_3O_4-NaAc	30.4	12.0	29.3	54.2	6.5	18.5	320	0.5	[1]
Fe_3O_4-NaOH	30.0	13.3	28.4	53.8	6.3	22.9	320	0.5	[1]
0.1Na/Fe_3O_4-pur	29.5	12.6	32.6	49.4	5.9	24.6	320	0.5	[1]
FeNa (0.43)	39.6	15.8	45.9	30.2	5.6	14.0	320	3.0	[2]
FeNa (1.18)	40.5	15.8	46.6	30.1	6.2	13.5	320	3.0	[2]
0.5Na/Fe	38.4	8.6	$76.8_{(C2+)}$		$5.3_{(C2+)}$	9.1	320	3.0	[3]
1Na/Fe	37.2	8.3	$77.1_{(C2+)}$		$5.3_{(C2+)}$	9.6	320	3.0	[3]
FeNa	42.1	29.7	34.6	28.5	4.8	15.2	340	2.0	[4]
0.5%Na	35.3	31.8	57.0*	--	5.7**	13.2	290	1.5	[5]
0.7%Na	34.1	30.4	58.4*	--	5.8**	12.5	290	1.5	[5]
0.9%Na	33.3	31.55	57.0*	--	5.7**	13.7	290	1.5	[5]
Na-Fe_3O_4	34.0	11.7	--	39.9	--	14.3	320	3.0	[6]

*C_2-C_7 olefins; **C_2-C_7 hydrocarbons.

REFERENCES

[1] Liu, B.; Geng, S.; Zheng, J.; Jia, X.; Jiang, F.; Liu, X., Unravelling the new roles of Na and Mn promoter in CO_2 hydrogenation over Fe_3O_4-based catalysts for enhanced selectivity to light α-olefins. *ChemCatChem* **2018,** 10 (20), 4718-4732.

[2] Wei, J.; Sun, J.; Wen, Z.; Fang, C.; Ge, Q.; Xu, H., New insights into the effect of sodium on Fe_3O_4-based nanocatalysts for CO_2 hydrogenation to light olefins. *Catal. Sci. Technol.* **2016,** *6* (13), 4786-4793.

[3] Liang, B.; Duan, H.; Sun, T.; Ma, J.; Liu, X.; Xu, J.; Su, X.; Huang, Y.; Zhang, T., Effect of Na promoter on Fe-based catalyst for CO_2 hydrogenation to alkenes. *ACS Sustain. Chem. Eng.* **2019,** *7* (1), 925-932.

[4] Xu, Y.; Zhai, P.; Deng, Y.; Xie, J.; Liu, X.; Wang, S.; Ma, D., Highly selective olefin production from CO_2 hydrogenation on iron catalysts: A subtle synergy between manganese and sodium additives. *Angew. Chem. Int. Ed.* **2020,** 59 (48), 21736-21744.

[5] Wei, C.; Tu, W.; Jia, L.; Liu, Y.; Lian, H.; Wang, P.; Zhang, Z., The evolutions of carbon and iron species modified by Na and their tuning effect on the hydrogenation of CO_2 to olefins. *Appl. Surf. Sci.* **2020,** 525, 146622.

[6] Wei, J.; Ge, Q.; Yao, R.; Wen, Z.; Fang, C.; Guo, L.; Xu, H.; Sun, J., Directly converting CO_2 into a gasoline fuel. *Nat. Commun.* **2017,** 8, 15174.